JOURNAL OF GEOPHYSICAL RESEARCH, VOL. 101, NO. B2, PAGES 3187–3198, FEBRUARY 10, 1996

Horizontal and vertical crustal movements from three-dimensional very long baseline interferometry kinematic reference frame: Implication for the reversal timescale revision

Kosuke Heki[1]

Kashima Space Research Center, Communications Research Laboratory, Kashima, Ibaraki, Japan

Abstract. Three-dimensional kinematic reference frame of geodetic very long baseline interferometry (VLBI) stations, tied to a geologic plate motion model, was established using the GLB907 solution by first selecting globally distributed stable plate interior stations and then applying a small translation and a rotation for the entire network in a three-dimensional space so that the differences in the "horizontal" velocities between the VLBI observations and the model predictions are minimized. Since the VLBI network is global, we only assume that the horizontal movements of tectonically stable stations obey a plate motion model; we need not introduce any unwarranted constraints to the vertical velocities of specific stations to realize the frame. A suggestive correlation was found between the estimated vertical velocities of North American stations and those predicted by a postglacial rebound model. The revision of the magnetic polarity timescale (MPTS) causes a uniform increase or decrease of the predicted velocities, which could be detected as the small difference between the measured and the predicted relative plate velocities. Direct estimation of the correction suggests that the VLBI data fit best to the model when the NUVEL1 model is corrected by +3.4% (± 1.2%), which differs significantly from the −4.5% deduced from the astronomical MPTS calibration. This was further confirmed by estimating the rotation rates for individual plate pairs.

Introduction

A set of time derivatives of the coordinates of space geodetic stations distributed worldwide, that is, a kinematic reference frame (KRF), would help us to connect local- or regional-scale geodynamic results with each other. A very long baseline interferometry (VLBI) observing session gives spot readings of the baseline vectors, vectors connecting VLBI stations. Series of these experiments yield relative displacements of points, which can be converted into site velocities through a certain inversion procedure.

The Goddard Space Flight Center (GSFC) data analysis group annually issues global solutions of geodetic VLBI (work by *Ma et al.* [1994a] is the last issue), which have been used as convenient data sets. Each report includes two different solutions: (1) the terrestrial reference frame (TRF) type solution, for example, the GLB907 solution of *Ma et al.* [1994a] and (2) the baseline evolution type solution, for example, the GLB908 solution of *Ma et al.* [1994a]. In the first solution, VLBI stations are modeled to move linearly with time and a set of geocentric coordinates and their time derivatives are given. In the second solution, site coordinates estimated as arc parameters for individual observing sessions give time evolutions of the baseline vector three components, namely, the length, the transverse, and the "vertical" components (called pseudovertical hereinafter because they are not really vertical). They correspond to length change, directional change equivalent to the horizontal movement of one station, and directional change perpendicular to the transverse component, respectively. The last pseudovertical component is really vertical only when a baseline is very short and becomes horizontal when the two ends of a baseline are antipodal (the length component, instead, becomes vertical). Average rates of change of each component are estimated by least squares fitting of a straight line to the time evolution of these components.

Many of the past studies of tectonic plate motions have been using such baseline evolution type VLBI data sets. Among them, *Argus and Gordon* [1990] directly estimated plate motion parameters (Euler vectors), while *Ward* [1990] and *Robaudo and Harrison* [1993a, b] first converted baseline evolution data to site velocities then estimated plate motion parameters. In these studies the pseudovertical baseline components have been excluded and the vertical site velocities have been fixed to zero for all the stations. These procedures are reasonable when treating relatively small areas and relatively short observing periods, but a more rigorous way has to be sought as the studied area becomes global and as we get more accurate changing rates for all the baseline vector components [*Robbins et al.*, 1993].

Systematic and random errors are the largest in the vertical component of a site coordinate to which VLBI is inherently insensitive [*Heki*, 1990]. In the weighted least squares method, a large "random" error of a datum is not a problem because a

[1]Now at Division of Earth Rotation, National Astronomical Observatory, Mizusawa, Iwate, Japan.

Paper number 95JB02845.
0148-0227/96/95JB-02845$05.00

reasonably small weight is given to it. Its "systematic" error, which comes largely from the atmospheric delays, is usually seasonal and can be considered to decrease with time. In fact, uncertainties of the pseudovertical baseline component changes in the last annual report [*Ma et al.*, 1994a] are almost equivalent to or sometimes better than the length changes in the report 4 years earlier [*Caprette et al.*, 1990].

Since the local vertical maps more into the length and less into the pseudovertical as the network becomes global [*Robbins et al.*, 1993], we might misunderstand baseline length changes due to vertical site movements as horizontal movements by wrongly fixing the vertical velocities to zero. The edge of the ancient Laurentide ice sheet is close to several important North American VLBI stations; for example, *James and Lambert* [1993] predicted an uplift of 3.9 mm/yr for the Canadian Algonquin VLBI station. This amount of uplift/subsidence could mislead us to believe that the trans-Atlantic plate velocity is ~10% faster/slower. Thus three-dimensional treatment of the KRF is important in discussing worldwide horizontal crustal movements as well as vertical movements.

In order to obtain three-dimensional KRF of VLBI stations, we could either (1) use all the three baseline components and estimate all the three site velocity components [*Sun and Zhao*, 1994] or (2) use the TRF type solution as the input data. Although the TRF solution lacks information on the nonlinear behavior of the baseline evolutions, it is irrelevant to the average velocities, and these two methods should give similar results. In this study I use the TRF type solution because that solution carries all correlations between experiments through into the final velocities while correlation between length changes of one baseline and another is unknown in the baseline evolution type solution. There are several stations where both VLBI and satellite laser ranging (SLR) are available. The combination of the data of the two techniques [*Robaudo and Harrison*, 1993a, b; *Sun and Zhao*, 1994] would improve the accuracy of the KRF, but the existence of independently established frames means that we can compare their results [*Watkins et al.*, 1994]. I therefore focus only on VLBI data in this study.

An astronomical approach to calibrate the ages of geomagnetic reversals has recently become available [*Shackleton et al.*, 1990; *Hilgen*, 1991a, b]. A new magnetic polarity timescale (MPTS) established astronomically by *Cande and Kent* [1992] reports ages for several recent reversals significantly older than the MPTS of *Harland et al.* [1982], which was used to derive the NUVEL1 plate motion model [*DeMets et al.*, 1990]. Thus *Gordon* [1993] and *DeMets et al.* [1994] proposed to revise the rotation rates in the NUVEL1 model downward by 4.4~4.5% and named the new model "NUVEL1a." Such a revision would appear as a small difference from unity, of the ratio between the geodetically measured relative plate velocities and the plate motion model predictions. The expected difference is well detectable with the currently available data of international geodetic VLBI and is going to be examined by applying the algorithm used to realize the KRF.

Algorithm

In VLBI it is necessary to constrain 6 degrees of freedom in order to remove the singularity that occurs when both site coordinates and Earth rotation parameters are estimated. Also this is the case for their time derivatives. When we estimate site velocities allowing the temporal changes of Earth rotation parameters, we have to constrain the rates of rotation and translation of the whole VLBI network. Here I compare two examples of past studies to obtain globally distributed site velocities using the minimal necessary constraints, which remove the singularity without introducing any additional and unwarranted constraints among the parameters.

Fallon and Dillinger [1992] fixed the sum of the velocities of all the stations and the net rotation of the network to arbitrary values. They then rotated and translated the network so that the arbitrary values coincide with the prediction by the no-net-rotation (nnr) NUVEL1 [*Argus and Gordon*, 1991] plate motion model. However, they did not discriminate stations by their tectonic setting, and so it is likely that the unmodeled velocities of several stations close to plate boundaries (e.g., Kashima, Japan and Mojave, California) have given errors to the applied translation and rotation and thereby affected the whole KRF.

Ma et al. [1994a], in contrast, trusted the velocities of a few selected "stable" stations to obtain the site velocities. Six velocity components were fixed to a priori values; the horizontal velocity (two components) of Westford (Massachusetts) and the change in direction of the vector from Westford to Richmond (Florida), to values predicted by the nnr-NUVEL1 [*Argus and Gordon*, 1991] model, and the vertical movements of Westford, Richmond, and Kauai (Hawaii) to zero. However, if either Westford or Richmond have finite horizontal movements relative to the North American plate or if any of Westford, Richmond, or Kauai have significant vertical movements, it will cause spurious rotation and translation of the KRF and a wrong rotation will result in larger errors far away from North America. In fact, the Westford station is suggested to move by 0.4, –0.5, and –1.5 mm/yr in the local east, north, and up directions with respect to the North American plate due to postglacial rebound [*James and Lambert*, 1993]. It is likely that the Westford-Richmond baseline is changing somewhat differently from the nnr-NUVEL1 prediction.

In the present study I use as many reference stations as possible in order to dilute the risk of degradation of the results by unexpected movements. At the same time, I choose only the "stable" stations (and the stable components) so that the obtained frame is least affected by the plate deformation. A certain uncertainty in the realization of the KRF may still remain due to the misfit between the measurements and the model predictions, even with stable reference stations. This uncertainty should be properly reflected in the final formal errors of the obtained site velocities. To satisfy these requirements, I first select a set of VLBI stations which have reliable velocity predictions (called "plate-fixed" stations hereinafter). Then I apply a small translation and a rotation for the entire network in a three-dimensional space so that the differences in the velocities between the VLBI observations and the model predictions are minimized in a weighted least squares sense.

Here a decision should be made whether we select plate-fixed stations from several plates or from a particular plate. The latter would mean that the frame is free from plate model errors, but their relatively small areal coverage would allow frame definition errors (random measurement errors and systematic errors arising from the unpredicted movements of plate-fixed stations) to grow in remote areas. The former, selecting globally distributed plate-fixed stations, is favorable from geometric point of view, but we have to pay attention to possible plate model errors. Another question is whether we should minimize the velocity difference just in the horizontal components or in the three components. Plate motion models predict only horizontal velocities and we do not have similar quantitative models for vertical movements. So the former is more logical. We should note, however, that determination of the rotation and translation with just the horizontal components is possible only when the site distribution is global. If we knew, in turn, vertical velocities by some other means, adjusting all the three components would offer a stronger geometric condition.

In this study I minimize horizontal velocity differences and select plate-fixed stations from multiple plates and name this KRF "the Global Frame." Other VLBI stations, located close to the plate boundaries, are called "free" stations. They nominally belong to certain major plates but are supposed to move with respect to their stable interiors. They do not contribute to the estimation of the rotation/translation (and the MPTS correction coefficient discussed later) of the entire network at all.

Now let $\mathbf{v}_i^{obs}$ and $\mathbf{v}_i^{prd}$ be the observed and predicted site velocities, $\mathbf{T}$ and $\mathbf{R}$ a translation and a rotation to be added and $\mathbf{r}_i$ the geocentric vectors to the VLBI stations. The observation equation is then

$$\mathbf{v}_i^{obs} = \mathbf{v}_i^{prd} + \mathbf{T} + (\mathbf{R} \times \mathbf{r}_i) + \mathbf{d}_i + \mathbf{e}_i \quad (i = 1, 2, \cdots, n), \qquad (1)$$

where $\mathbf{e}_i$ is the measurement error of the velocity of ith station and $\mathbf{d}_i$ is the velocity of the ith point with respect to the plate motion model. The value n is the total number of stations that includes n_{fix} plate-fixed stations ($n_{\text{fix}} < n$). The difference between the plate-fixed and free stations lies in the components of the $\mathbf{d}_i$,

$$\mathbf{d}_i = \begin{pmatrix} 0 \\ 0 \\ d_i^u \end{pmatrix} \quad (i = 1, 2, \cdots, n_{\text{fix}})$$

$$\mathbf{d}_i = \begin{pmatrix} d_i^n \\ d_i^e \\ d_i^u \end{pmatrix} \quad (i = n_{\text{fix}} + 1, \cdots, n). \qquad (2)$$

Now we estimate M parameters,

$$M = n_{\text{fix}} + 3(n - n_{\text{fix}}) + 6,$$

where the first and the second terms correspond to the $\mathbf{d}_i$ of the plate fixed and free stations, the third term to the $\mathbf{T}$ and $\mathbf{R}$, with the weighted least squares method. We have N data,

$$N = 3n.$$

The values of $\mathbf{v}^{prd}$ can be easily calculated using the nnr-NUVEL1 model and, by correcting them by –4.5%, we can replace the original nnr-NUVEL1 with the "nnr-NUVEL1a." Values of $\mathbf{v}^{obs}$ and $\mathbf{r}$ are available in the GLB907 solution and its machine readable version offers the original full covariance matrix $\mathbf{Q}_0$,

$$\mathbf{Q}_0 \equiv \langle \mathbf{E}\widetilde{\mathbf{E}} \rangle, \qquad (3)$$

where $\mathbf{E} \equiv (e_1^x, e_1^y, e_1^z, \cdots, e_n^x, e_n^y, e_n^z)$. The errors of the six velocity components, fixed to remove the rank defficiency, are set to zero in the original GLB907 covariance matrix. First we add a covariance matrix $\mathbf{\Sigma}_{\text{trans/rot}}$ to this in order to remove these constraints. Its translation part is designed so that each component is 100% correlated among the stations to represent the translational uncertainty of the whole network. Its rotation part is designed likewise so that it represents the rotational uncertainty. The intersite correlations cancel the changes in the variances of quantities that should be invariant to rotation and translation, that is, baseline length changing rates and the rates of changes of the angles between baselines. By the same reason, this addition does not affect the determination of the σ_{add} (explained below). Its influence on the estimated translation and rotation is fairly small (less than 1% of the lengths of the estimated $\mathbf{T}$ and $\mathbf{R}$), but it does increase the formal errors of the estimated parameters to some extent. Such translational/rotational uncertainty was set equivalent to the σ_{add} throughout this study.

The postfit velocity residuals are expected to be as large as their measurement errors if the plate model is correct and plate interiors are rigid. However, uncertainties of the model (including those due to the MPTS error) and the occurrence of intraplate earthquakes suggest this is not the case. I therefore assume that the horizontal velocities of the plate-fixed stations "almost" obey the plate motion model, and I determine the contribution of such model defects a posteriori. I add another covariance matrix $\mathbf{\Sigma}_{\text{add}}$ that represent isotropic errors without intersite correlation, so that the reduced χ^2 becomes unity, namely,

$$\text{reduced } \chi^2 \equiv \frac{\widetilde{\mathbf{V}}_{\text{res}}(\mathbf{Q}_0 + \mathbf{\Sigma}_{\text{trans/rot}} + \mathbf{\Sigma}_{\text{add}})^{-1}\mathbf{V}_{\text{res}}}{(N - M)} \simeq 1, \qquad (4)$$

where $\mathbf{V}_{\text{res}}$ is the vector composed of the postfit residual velocities of n stations (they are zero for free stations because the velocity $\mathbf{d}_i$ is designed for each of them). $\mathbf{\Sigma}_{\text{add}}$ is a diagonal matrix whose components σ_{add}^2 correspond to the additional isotropic error to be determined a posteriori to satisfy the condition in (4). By its definition, σ_{add} should be much smaller than the plate motion itself, say less than a few millimeters per year.

This readjustment does not alter the GLB907 KRF in a relative sense at all; the rotation and translation applied here preserve the nature of the original GLB907 that it minimizes the residuals of the VLBI delay observables. This was possible because the original GLB907 is a minimal constraint solution, that is, only sufficient parameters to remove the rank deficiencies were fixed. Similar ideas can be found in the deformation analysis using terrestrial geodetic survey data. Giving the nnr-NUVEL1 velocities as $\mathbf{v}^{prd}$ corresponds to the "model coordinate solution" of *Segall and Matthews* [1988], and an idea similar to the classification of points into plate-fixed and free stations is given by *Gu and Prescott* [1986].

Establishment of the Kinematic Reference Frame

Global Frame

The plate-fixed VLBI stations were selected only from fixed, permanent VLBI stations located in stable plate interiors, which I define as areas more than 500 km from the nearest plate boundary. A smaller distance would increase the risk of the result being affected by variable deformation rates in the plate boundary zones, but too few stations would be left in plate "interiors" with a larger threshold. The following 16 stations are taken from four tectonic plates to establish the Global Frame. From the North American plate, seven stations, namely, Westford and Haystack (Massachusetts), Richmond (Florida), Green Bank ("NRAO 140", Virginia), Maryland Point (Maryland), Algonquin (Ontario), and Fairbanks ("GILCREEK," Alaska) are selected. I selected Wettzell, Effelsberg (both in Germany), Madrid ("DSS65" Spain), Onsala (Sweden), from the Eurasian plate, Kauai (Hawaii), Kwajalein (Marshall Islands), and Minamitorishima (Marcus Island, northwestern Pacific Ocean) from the Pacific plate, Tidbinbilla ("DSS45," Canberra) and Hobart (Tasmania) from the Australian plate. They have sufficiently numerous measurements over sufficiently long periods of time.

Hartbeesthoek (South Africa) is excluded because it lies just on the boundary between the original African plate and the Somalian plate [*Jestin et al.*, 1994]. Shanghai (China) is not used either because the complicated tectonics in Central and Eastern Asia [*Molnar and Tapponnier*, 1975] makes it difficult to establish kinematic models for minor crustal blocks in Asia. Other VLBI stations including those with long observational histories, for example, Kashima (Japan), Mojave (California), and Matera (southern Italy), are all treated as free stations. I found 47 free stations whose velocities have been independently determined in the GLB907 solution.

If the plate-fixed stations are uniformly distributed on the Earth, all components of $\mathbf{T}$ and $\mathbf{R}$ would be well distinguished; that is, their between-parameter correlations would be small. In the present case the largest correlation was as small as 62% (between the T_y and R_x) and every component was estimated with sufficient accuracy. The 1σ formal errors of T_y and R_x were 1.07 mm/yr and 2.0×10^{-10} rad/yr, respectively; the latter corresponds to ~1 mm/yr on the Earth's surface. The lengths of the estimated $\mathbf{T}$ and $\mathbf{R}$ were 3.7 mm/yr and 4.5×10^{-10} rad/yr, respectively. The latter corresponds to the maximum movement on the Earth's surface of ~2.9 mm/yr. In order to satisfy (4), I added the σ_{add} of 0.67 mm/yr, which corresponds to plate interior deformations and errors in the plate motion model. This is much smaller than typical plate speeds, which justify the assumption that the horizontal velocities of the plate-fixed stations "almost" obey the plate motion model.

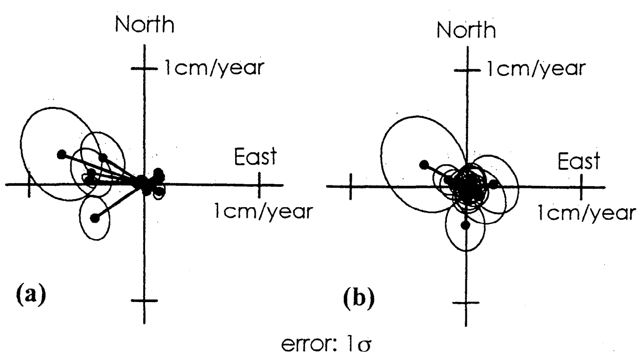

Figure 1. Residuals of the horizontal velocities of the 16 plate-fixed VLBI stations in the Global Frame. Two figures show (a) those before the application of translation/rotation (i.e., raw velocities in GLB907 [*Ma et al.*, 1994a]) and (b) after the readjustment of the kinematic reference frame. Plotted 1σ errors are taken from GLB907 (Figure 1a) but certain errors are added in Figure 1b (see text).

Figures 1a and 1b show the residual velocities plotted for the 16 plate-fixed stations before and after the readjustment of the KRF. Westward deviated velocity residuals in Figure 1a, possibly originating from the errors in the six velocity components fixed in the original solution, disappear after the readjustment in Figure 1b (these residuals are summarized in Table 1). The weighted root-mean-squares (WRMS), that is, the weighted average of the postfit residuals, is 0.75 and 0.79 mm/yr for the north-south and east-west components, respectively, an order of magnitude smaller than ~5 mm/yr derived by *Fallon and Dillinger* [1992], in which no discrimination has been made for stable and unstable stations. These small residuals suggest that plate velocities are highly consistent between geodetic (the last decade) and geological (the last few Ma) time windows.

Vertical Velocities and Postglacial Rebound

In Table 1 I summarize the residual horizontal velocities (those plotted in Figure 1b) and the estimated vertical components of $\mathbf{d}_i$ for plate-fixed stations, and the three components of the $\mathbf{d}_i$ for the free stations. Since $\mathbf{v}_i^{prd}$ are calculated by assuming plates listed in Table 1 for free stations, the $\mathbf{d}_i$ are relative to the stable parts of these plates. Figure 2 compares the vertical components of $\mathbf{d}_i$ in Table 1 with the predictions of a postglacial isostatic rebound model for North America and Europe [*James and Lambert*, 1993]. These predictions were obtained assuming the ICE-3G deglaciation chronology [*Tushingham and Peltier*, 1991] and an appropriate rheology for the mantle. In North America, the observed and predicted vertical velocities suggest some correlation, that is, the postglacial rebound might be detected by VLBI.

Little correlation is seen, on the other hand, in Europe. Out of the three (Onsala, Effelsberg, and Wettzell) stations with sufficiently small errors, Onsala shows an agreement while the other two German stations show subsidences of 5–6 mm/yr (their predicted subsidences are < 1 mm/yr). Possible explanations for this include (1) subsidence related to the Rhine graben, (2) local subsidence due to mechanical problems, (3) unknown processes deep in the mantle, and (4) the error of the plate motion model adopted as the reference. The effect of the MPTS revision is not responsible because replacing NUVEL1 with NUVEL1a does not change the estimated Wettzell subsidence by more than 1 mm/yr. *Ma et al.* [1994b] obtained the vertical movement of -4.6 ± 0.4 mm/yr for Wettzell (negative value indicates subsidence) with a similar VLBI data set but by fitting straight lines to the vertical positions estimated session by session. SLR data from 1984 to 1991 [*Dunn et al.*, 1993] suggest the vertical velocity of Wettzell of −1.5 mm/yr but, due to its large error of ±3.0 mm/yr, it does not support nor oppose the VLBI results.

Kato [1983] isolated secular components out of monthly mean sea level data at various tide gauge stations in Japan and found that they can be classified into nine regions by their trends. The "region II," the whole eastern coast of northeast Honshu including Kashima, is characterized by the sea level rise of ~5 mm/yr. A tide gauge station at the Kashima port, a few kilometers from the VLBI station, shows sea level rise of 7.1 mm/yr from 1969 to 1993 [*Geographical Survey Institute*, 1994]. Because the global sea level rise is not much faster than 1–2 mm/yr [e.g., *Douglas*, 1991], subsidence with an amount similar to the sea level rise is expected at the Kashima VLBI station. The vertical velocity of Kashima obtained in this

Table 1. Velocity of VLBI Stations With Respect to the Plates

Site	Plate	Position: Latitude, deg	Position: Latitude, min	Position: Longitude, deg	Position: Longitude, min	Velocity and Errors: North, mm/yr		Velocity and Errors: East, mm/yr		Velocity and Errors: Up, mm/yr		Correlation, %: North-East	Correlation, %: East-Up	Correlation, %: Up-North
Plate-Fixed Stations														
Algopark	na	45	57	281	56	−0.8	1.2	0.2	1.2	4.4	1.2	0.1		
Dss45	au	−35	23	148	59	−0.8	2.4	1.2	2.2	6.5	2.6	−23.3		
Dss65	eu	40	26	355	45	−1.0	1.3	0.1	1.3	−9.9	2.7	3.7		
Eflsberg	eu	50	31	6	53	0.7	1.3	0.4	1.2	−6.9	1.1	0.4		
Gilcreek	na	64	59	212	30	−0.5	1.2	0.7	1.2	−0.3	0.8	1.0		
Haystack	na	42	37	288	31	−0.1	1.2	0.5	1.2	1.1	0.9	0.1		
Hobart26	au	−42	47	147	26	0.2	2.5	2.3	2.2	6.9	2.8	−21.7		
Kauai	pa	22	8	200	20	0.6	1.3	−1.6	1.3	1.6	0.9	−13.1		
Kwajal26	pa	9	24	167	29	−3.3	2.2	−0.1	1.7	2.7	4.7	−6.9		
Marcus	pa	24	17	153	59	1.9	4.1	−3.7	3.7	24.0	13.4	−19.3		
Marpoint	na	38	22	282	46	0.2	1.2	0.0	1.2	−1.4	2.2	0.5		
Nrao 140	na	38	26	280	10	0.3	1.2	−0.3	1.2	1.1	1.0	0.1		
Onsala60	eu	57	24	11	56	0.2	1.3	−1.1	1.2	0.1	0.9	0.3		
Richmond	na	25	37	279	37	0.6	1.2	0.3	1.2	2.9	0.9	0.2		
Westford	na	42	37	288	30	−0.3	1.2	0.1	1.2	2.1	0.8	0.0		
Wettzell	eu	49	9	12	53	0.4	1.3	0.5	1.2	−5.4	0.9	0.9		
Free Stations														
Blkbutte	na	33	40	244	17	4.1	1.4	−6.8	1.1	−7.4	9.0	−9.5	7.6	−13.7
Deadmanl	na	34	15	243	43	3.0	4.1	−7.1	2.9	63.2	24.1	10.2	−2.5	−29.2
Dss15	na	35	25	243	7	8.9	3.6	−2.5	2.6	−2.5	11.1	30.9	31.2	45.5
Ely	na	39	18	245	9	0.6	1.2	−3.9	1.0	−4.5	6.5	−9.8	8.9	−19.7
Fd-vlba	na	30	38	256	3	8.2	2.0	−2.5	2.1	15.3	9.3	16.7	−3.5	15.7
Flagstaf	na	35	13	248	22	0.7	1.2	−1.2	1.0	15.1	6.4	−2.5	3.9	3.3
Fort ord	pa	36	40	238	14	−1.4	1.1	−1.4	1.0	11.5	6.1	−1.8	−5.2	−8.3
Goldvenu	na	35	15	243	12	7.9	0.8	−4.5	0.8	−1.9	1.4	2.2	10.0	15.9
Gorf7102	na	39	1	283	10	2.8	1.3	0.8	1.1	24.4	5.9	−0.4	−5.2	−4.3
Hartrao	af	−25	52	27	41	−9.5	1.6	−4.4	1.6	−1.9	1.8	−9.8	−25.9	47.6
Hatcreek	na	40	49	238	32	6.2	0.8	−6.7	0.8	1.4	1.2	1.9	5.2	7.6
Jpl mv1	pa	34	12	241	50	−15.0	1.0	2.9	0.9	9.5	5.6	−2.5	−6.9	−8.3
Kashima	eu	35	57	140	40	2.8	0.9	−20.5	0.9	−5.0	1.1	1.4	20.9	18.2
Kodiak	na	57	44	207	30	6.6	1.1	−4.7	1.2	16.6	7.2	−3.4	13.7	−12.8
La-vlba	na	35	47	253	45	3.7	0.9	−2.1	0.9	−3.5	2.3	1.5	1.6	10.4
Mammothl	na	37	38	241	3	11.0	2.4	−12.6	1.6	−16.9	14.7	−16.0	0.0	−17.7
Matera	eu	40	39	16	42	3.8	1.0	2.6	1.0	−1.7	2.9	−0.1	−15.1	13.2
Medicina	eu	44	31	11	39	1.5	0.8	2.2	0.8	−9.1	1.3	−0.1	−13.6	8.8
Mojave12	na	35	20	243	7	8.3	0.7	−4.3	0.7	−1.0	0.8	0.1	5.3	12.7
Mon peak	pa	32	54	243	35	−9.3	0.9	−1.1	0.8	−3.3	3.3	1.2	7.5	1.8
Nome	na	64	34	194	38	−4.3	1.3	4.3	1.0	10.4	6.1	−18.1	16.0	−15.2
Noto	eu	36	53	14	59	6.5	1.0	−0.7	1.0	−6.6	2.8	2.9	−13.4	16.5
Nrao85 3	na	38	26	280	9	1.9	0.8	−3.2	0.7	3.7	1.2	−0.5	−6.0	7.4
Ovro 130	na	37	14	241	43	8.9	0.8	−6.6	0.8	0.0	1.2	0.8	10.4	16.0
Pblossom	pa	34	31	242	5	−18.9	1.3	12.2	1.0	−9.8	7.9	−4.6	7.1	−13.4
Pentictn	na	49	19	240	23	1.7	1.2	1.4	1.1	26.7	8.6	−2.9	−7.5	−16.2
Pietown	na	34	18	251	53	−0.1	0.8	−2.2	0.8	−7.9	1.3	0.0	5.9	11.1
Pinflats	na	33	37	243	32	18.4	1.0	−17.7	0.9	1.7	5.2	−2.6	9.0	0.9
Plattvil	na	40	11	255	16	−0.9	0.9	−0.4	0.8	4.1	3.7	3.2	−10.8	−6.0
Presidio	pa	37	48	237	33	−14.3	1.1	7.5	0.9	−1.6	5.5	−0.5	−1.0	−8.2
Pt reyes	pa	38	6	237	4	−6.9	1.0	3.4	0.9	13.0	4.5	0.3	−8.4	4.8
Pverdes	pa	33	45	241	36	−8.2	1.3	2.1	1.1	−7.6	8.6	3.4	−10.5	−11.1
Quincy	na	39	58	239	3	7.1	0.9	−9.0	0.8	−2.0	3.7	1.7	3.6	−9.5
Robled32	eu	40	26	355	45	−0.7	0.8	0.1	0.8	−9.9	2.7	1.3	11.1	27.6
Sanpaula	pa	34	23	241	0	−11.9	1.3	1.7	1.1	12.0	8.4	−6.5	−1.0	−12.4
Seattle1	na	47	41	237	45	2.4	2.1	0.9	1.7	−19.5	13.7	−0.4	19.3	−14.9
Seshan25	eu	31	6	121	12	−4.2	1.2	10.3	1.2	−5.8	3.1	1.6	11.2	0.6
Sndpoint	na	55	21	199	31	0.4	1.2	−5.0	1.7	4.4	8.7	−15.2	36.1	−20.2
Tromsono	eu	69	40	18	56	0.1	1.3	9.8	1.6	−4.8	6.6	−12.0	−0.7	−18.2
Tsukuba	eu	36	6	140	5	2.7	1.4	−20.5	1.3	−5.1	4.4	0.1	6.2	1.0
Vernal	na	40	20	250	26	−0.4	1.4	2.3	1.1	14.2	8.0	1.0	−5.7	−14.1
Vndnberg	pa	34	33	239	23	−2.4	0.8	−0.1	0.8	3.6	1.2	0.0	5.7	6.8
Whthorse	na	60	43	224	55	14.6	3.0	0.2	2.8	−86.1	22.6	18.2	−8.8	−11.5
Yakataga	na	60	5	217	31	28.9	1.5	−21.1	1.8	38.9	10.5	25.4	9.3	−5.0
Yellowkn	na	62	29	245	32	0.8	0.9	1.1	0.8	10.2	3.4	−2.1	6.4	2.1
Yuma	na	32	56	245	48	1.2	1.1	−1.2	0.9	18.0	6.2	−0.8	1.6	−3.5

Abbreviations are na, North America; eu, Eurasia; pa, Pacific; au, Australia; af, Africa. VLBI site names follow *Ma et al.* [1994a]. Errors are 1σ

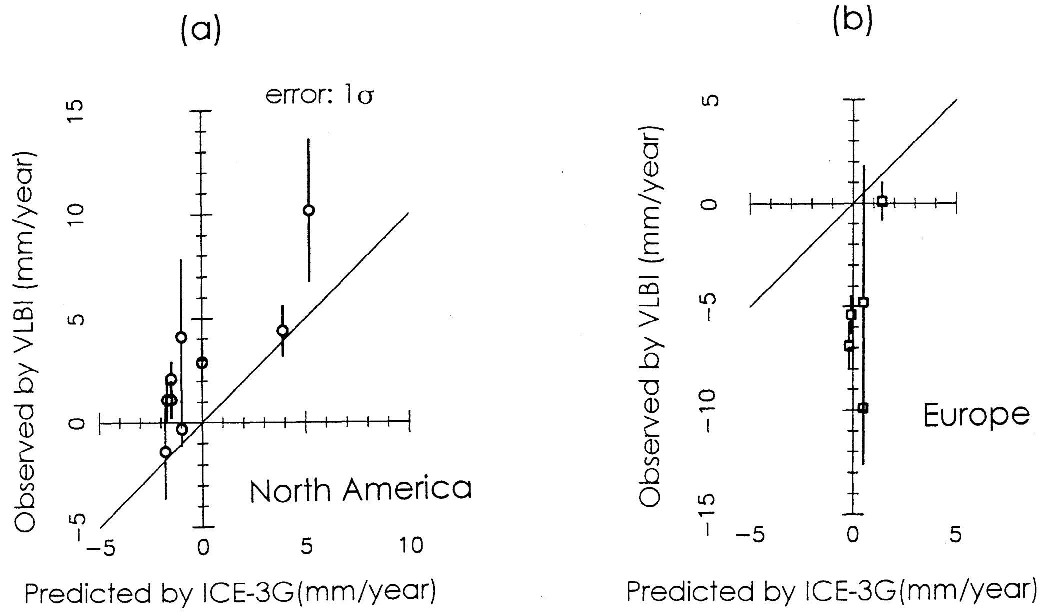

Figure 2. Comparison between the vertical velocities in Table 1 and those predicted by *James and Lambert* [1993] for (a) North America and (b) Europe. The figure includes all the stations whose predictions are available except those whose vertical velocity errors (Table 1) are larger than 5 mm/yr. Errors are 1σ. The data would lie along the solid lines if the observations and the predictions are consistent.

study is plotted and compared with sea level data in Figure 3. Its subsidence of 5.0±1.1 mm/yr (when the original NUVEL1 velocities were used) is significantly different from zero but is consistent with the general long-term trend of multiple tide gauge stations (including the one at Kashima) along the Pacific coast of northeast Japan, over the last few decades.

Two other data in Figure 3 show the vectors obtained by employing different MPTS correction coefficients for the NUVEL1 model. One of them is the -4.5% correction as suggested by *DeMets et al.* [1994], and the other is the +3.4% correction which minimizes the differences between the VLBI velocities and the model predictions (discussed in the next

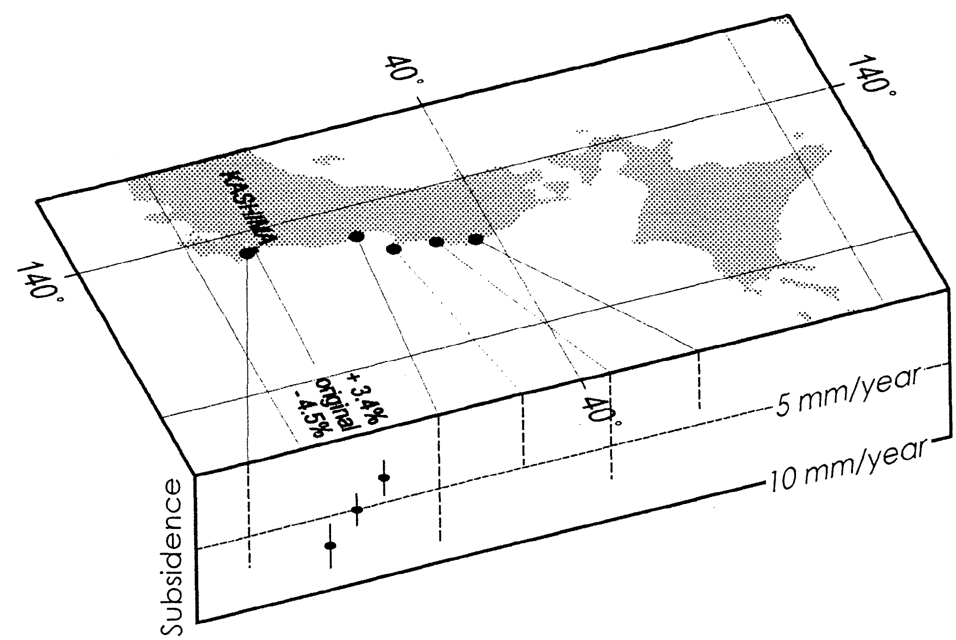

Figure 3. Downward component of the velocity of Kashima is shown with solid lines with error bars indicating 1σ formal errors. The three data points correspond to the vectors based on the original NUVEL1 (labeled as "original"), the NUVEL1 model modified by -4.5% (i.e., NUVEL1a; "-4.5 %"), and by +3.4% (best estimate obtained in this study; "+3.4%"). Sea level rise rates are given as dashed vertical bars extending downward for the five tide gauge stations indicated with solid circles in the map, that is, Kashima, Soma, Ayukawa, Ofunato, and Miyako (from south to north). They are classified into the same region by *Kato* [1983] and the latest rate data are taken from *Geographical Survey Institute* [1994].

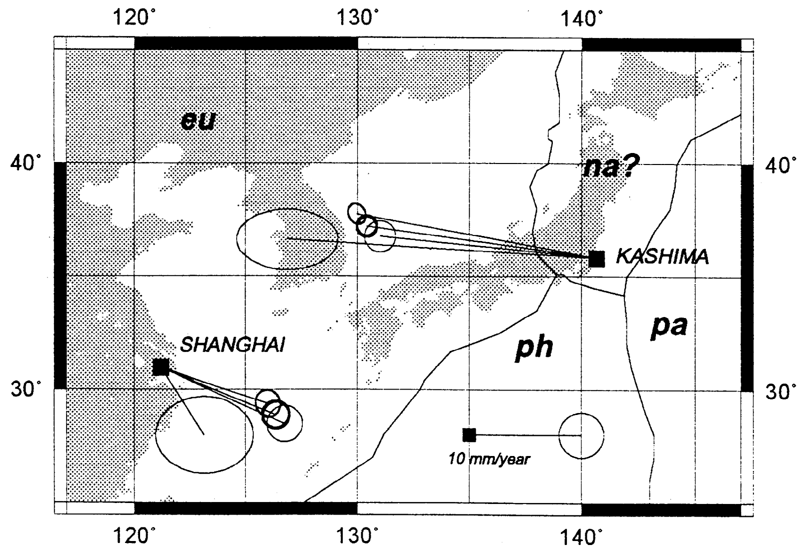

Figure 4. Horizontal displacements of Shanghai and Kashima with respect to the stable interior of the Eurasian plate. Three vectors with relatively small error ellipses, for each of them, are obtained by the same way as in Figure 3. The vector with the error ellipse drawn with the thickest line is based on the original NUVEL1, while the second thickest and the thin ones correspond to those corrected by +3.4% and by -4.5%, respectively. The two vectors with larger error ellipses are those estimated together with the North America–Eurasia Euler vector (see text). Error ellipses are all 1σ. Abbreviations for the plates are as follows: eu, Eurasian plate; na, North American plate; pa, Pacific plate; and ph, Philippine Sea plate.

main section). Figure 3 shows that a plausible amount of the correction coefficient of the MPTS does not seriously influence the estimated vertical velocities. The vertical velocity of the nearby Shanghai station was as large as Kashima (-5.8 ± 3.1 mm/yr), but I do not discuss it in this study because it is not siginificantly different from zero (i.e., $< 2\sigma$) nor have we a long tide gauge record close to this station for comparison.

Horizontal Velocities of the Free Stations

An important condition to obtain the horizontal velocity of a certain station close to the plate boundary with respect to the stable interior of that plate would be to define a KRF with the reference stations located on the interior of that plate and to confirm that this network is deformation-free. The present site distribution and the observation history of VLBI makes this difficult except for the North American plate. Two vectors in Figure 4 with the largest errors for Shanghai and Kashima are their velocities relative to the Eurasian interior obtained by rigorously interpreting the above "condition." They are obtained by first establishing the "North American Frame (No. 1)" (explained in detail in the next main section), then by estimating the three components of the North American–Eurasian Euler vector using Wettzell, Effelsberg, Madrid, and Onsala together with the horizontal velocities of Kashima and Shanghai. Their large errors, which come from the weak geometric condition of the four reference stations, linearly distributed over a relatively small area, makes it difficult to use these data for tectonic studies.

In the previous section I showed that, by translating and rotating the GLB907 velocities a little, and by adding an isotropic error of 0.67 mm/yr, the horizontal movements of all the plate-fixed stations became consistent (i.e., the residuals are as large as the errors) with the NUVEL1 plate motion model. I regard this the satisfaction of the "condition," then the horizontal components of $\mathbf{d}_i$ of free stations can be interpreted as their movements with respect to the plate interiors. They are shown in Figure 4 as vectors with relatively small error ellipses drawn with thick lines. They are accurate to 1~2 mm/yr and useful for tectonic studies. The other two vectors for each of Kashima and Shanghai are obtained by adopting two modified NUVEL1 models, that is, the -4.5% correction by astronomical calibration of the MPTS [*DeMets et al.*, 1994] and the +3.4% correction that I propose in this study. Their 1σ error ellipses overlap with each other, and we may conclude that the error due to the MPTS uncertainty is not so serious as to call for different tectonic interpretations for these vectors.

Now I compare the velocity vector of Shanghai of ~1 cm/yr toward east-southeast (N112.2°E, 11.1 mm/yr) with those inferred by other means. There is a classical hypothesis that the northward movement of the Indian subcontinent, after its collision with Eurasia, has been partly accommodated by the eastward extrusion of crustal blocks in eastern Asia [*Molnar and Tapponnier*, 1975]. In spite of a controversy on the partition of strain produced by the Indian-Asian collision between crustal thickening and eastward displacement [*Avouac and Tapponnier*, 1993; *Houseman and England*, 1993], there is a rough agreement on the current extrusion rate of southern China. Geological estimates of shortening and slip rates in thrust zones and strike-slip faults suggest that the western edge of the South China block is moving east-southeastward by 10–15 mm/yr [*Avouac and Tapponnier*, 1993]. Geophysical numerical experiments based on a thin viscous sheet model of the lithosphere also predict a similar rate with minor variation due to geometry or rheology [*Houseman and England*, 1993]. Shanghai's horizontal velocity derived here agrees with these two inferred velocities and also with the recent study based on earthquake strain rates in central and eastern Asia [*Holt et al.*, 1995].

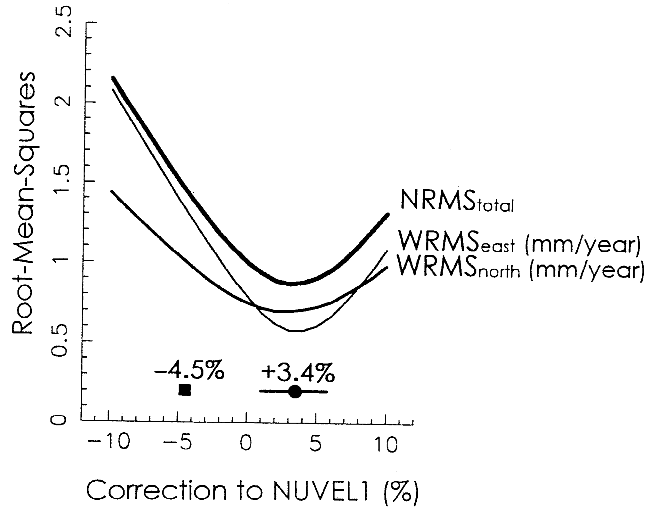

Figure 5. Three curves showing the behaviors of the root-mean-squares when various correction coefficients were given to the original NUVEL1 model. Variable σ_{add} is fixed to the same value. The thickest line and two thinner lines correspond to the total normalized root-mean-squares (NRMS) and the weighted root-mean-squares (WRMS), respectively. NRMS is the square root of the reduced χ^2 in (4) and WRMS is the weighted average of the postfit residuals. The estimated value and its 2σ error bar is plotted below, together with the position of the -4.5% a priori correction.

Geomagnetic Reversal Timescale Revision

Direct Estimation of the Revision Coefficient

A new astronomical approach to calibrate the ages of geomagnetic polarity reversals [*Shackleton et al.*, 1990; *Hilgen*, 1991a, b] and the revision of MPTS by *Cande and Kent* [1992] that followed suggest that all the plate rotation rates in the NUVEL1 relative plate motion model [*DeMets et al.*, 1990] should be revised downward by -4.4~4.5% [*Gordon*, 1993; *DeMets et al.*, 1994]. Incorporation of such a revision factor can be easily performed in the present method to establish a KRF, by modifying the observation equation (1) to

$$\mathbf{v}_i^{obs} = (1+\alpha)\mathbf{v}_i^{prd} + \mathbf{T} + (\mathbf{R} \times \mathbf{r}_i) + \mathbf{d}_i + \mathbf{e}_i, \quad (5)$$

where α is the timescale correction coefficient. I call the -4.5% astronomical correction ($\alpha = -0.045$) the "a priori correction."

Figure 5 shows how the root-mean-squares of the 16 plate-fixed stations behave according to the change of α. There I use the same σ_{add} (i.e., 0.67 mm/yr). The thick curve shows the normalized root-mean-squares (NRMS), the square root of the reduced χ^2 in (4). It is unity when α is zero; that is, the original NUVEL1 is used. The two thinner curves indicate the WRMS in the two horizontal velocity components. None of them show minima at the a priori correction of -4.5% but they suggest that the fit becomes best when the NUVEL1 velocities are modified faster by +3~4%. Figure 6a shows the horizontal velocity residuals when the a priori correction has been given.

As the next step, the α was estimated as a parameter together with $\mathbf{T}$ and $\mathbf{R}$. The maximum correlation between α and the components of $\mathbf{T}$ and $\mathbf{R}$ was 48%; the α is well distinguishable as an independent parameter. The σ_{add} that satisfies (4) has decreased to 0.56 mm/yr. The estimated α was +3.4% with the 1σ formal error of ±1.2%, which is significantly different from the a priori correction (Figure 5). The fit of the horizontal velocities is much improved by this "space geodetic calibration of MPTS" as shown in Figure 6b. This suggests that the NUVEL1 is not too fast but is too slow and needs to be revised upward by 3.4% as far as the worldwide geodetic VLBI data of 1979–1992 are concerned.

North American Frame and the Estimation of Euler Vectors

In order to further confirm the results of the previous section, I estimate the Euler vectors of several plate pairs. Because the Global Frame uses the NUVEL1-derived information in its establishment, it is unsuitable for this purpose. I therefore introduce the "North American Frame" here. Seven stations indicated as "na" in Table 1 are used as the plate-fixed stations and I treat other "plate-fixed" stations as free stations. By calculating $\mathbf{v}_i^{prd}$ for all the stations assuming the North American plate and by performing the same weighted least squares estimation, $\mathbf{d}_i$ for the free stations can be estimated as the velocities relative to the North American plate.

Now we have only a regional distribution of the plate-fixed stations, we need to use the vertical velocities as well as the horizontal components to estimate both $\mathbf{T}$ and $\mathbf{R}$. Possible correlation between the observations and the predictions for the vertical velocities in North America (Figure 2a) makes it reasonable to adopt these predictions for the vertical components of $\mathbf{v}_i^{prd}$. I call this the North American Frame No. 1. The same weighted least squares calculation as the Global Frame has been performed by including the ICE-3G velocities [*James and Lambert*, 1993] in $\mathbf{v}_i^{prd}$ and modifying (2) to

$$\mathbf{d}_i = \begin{pmatrix} 0 \\ 0 \\ 0 \end{pmatrix} \quad (i = 1, 2, \cdots, n_{\text{fix}})$$

$$\mathbf{d}_i = \begin{pmatrix} d_i^n \\ d_i^e \\ d_i^u \end{pmatrix} \quad (i = n_{\text{fix}} + 1, \cdots, n). \quad (6)$$

Figure 7 shows the velocity residuals for the seven plate-fixed stations. Because all three components were adjusted, vertical velocity residuals are plotted there as well.

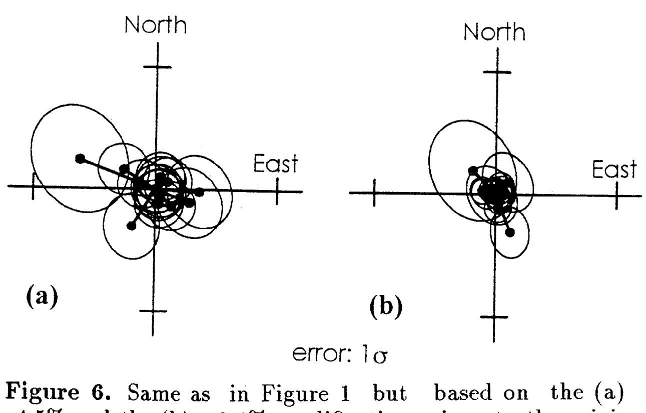

Figure 6. Same as in Figure 1 but based on the (a) -4.5% and the (b) +3.4% modifications given to the original NUVEL1 velocities. The WRMS in the north and east components for the two cases are (a) 1.06 and 1.56 mm/yr and (b) 0.66 and 0.56 mm/yr.

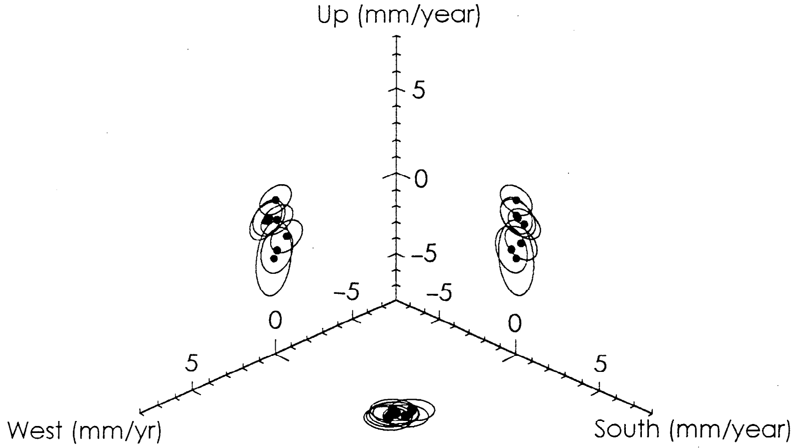

Figure 7. Residual velocities in three components for the seven plate-fixed stations in North America for the "North American Frame (No. 1)," in which all the three components were minimized by translating/rotating the original KRF. Velocities caused by postglacial rebound [*James and Lambert*, 1993] are included in the predicted velocities. The WRMS of the three components are 0.25, 0.39, and 1.01 mm/yr in the north, east, and up axes, respectively. The residuals and the 1σ error ellipses are projected onto three planes perpendicular to each other.

I try an additional case (the North American Frame No. 2) where we estimate only **R** and leave **T** fixed to zero. In this case we do not have to adjust the vertical rates since they do not contribute to the determination of **R**. The advantage is that we do not rely on the predicted vertical velocities in North America. A drawback is that, if there are nonzero rates in Westford and Richmond verticals which were fixed to zero in the GLB907, they would affect the horizontal movement of sites far from North America. This KRF can be obtained using the same equations as the Global Frame with the three components of **T** fixed to zero.

With the velocities of two or more sites in the stable interior of a certain plate viewed from another plate, we could estimate the instantaneous rotation vector (Euler vector) between the plates by the linear inversion [*Ward*, 1990]. This was the case between the North American plate and the three plates, namely, the Eurasian plate (Onsala, Wettzell, Effelsberg, and Madrid), the Pacific plate (Kauai, Kwajalein, and Minamitorishima) and the Australian plate (Tidbinbilla and Hobart).

Table 2 summarizes the three components of the Eurasia-North America and the Pacific-North America Euler vectors estimated using the two North American frames, and Figure 8 compares them with the NUVEL1 [*DeMets et al.*, 1990] and RM2 [*Minster and Jordan*, 1978] pole positions. The North America–Eurasia (na–eu) poles are less accurate than the North America–Pacific (na–pa) poles, due to the poor geometry of the four Eurasian plate stations. Euler pole position was not estimated for the North America–Australia pair (na–au) because the two Australian stations are too close to enable such an estimation with a meaningful accuracy. Rotation rates estimated for the na–eu and na–pa pairs in this way are shown as open squares in Figures 9a and 9b. For the above three plate pairs, I estimated the Euler vector lengths fixing their directions so that meaningful accuracies are obtained for all the three plate pairs (open circles in Figure 9). The results are fairly different from the a priori correction of –4.5% and show rates faster than the original NUVEL1 rotation rates by a few percent, that is, the same conclusion as the previous section can be drawn.

Table 2. Estimated Euler Vectors

Plate Pair	ω_x	ω_y	ω_z	$C_{x,y}$	$C_{y,z}$	$C_{z,x}$	$\lvert\omega\rvert$	$\lvert\omega_0\rvert$
North American Frame 1								
na-eu*	–	–	–	–	–	–	0.234 ± 0.006	0.22 ± 0.01
na-eu	–0.047 ± 0.027	0.079 ± 0.007	0.242 ± 0.031	45.2	45.7	96.7	0.259 ± 0.026	–
na-pa*	–	–	–	–	–	–	0.810 ± 0.011	0.78 ± 0.01
na-pa	–0.131 ± 0.029	0.507 ± 0.010	–0.617 ± 0.015	52.1	–38.4	–66.6	0.809 ± 0.012	–
na-au*	–	–	–	–	–	–	0.828 ± 0.018	0.79 ± 0.01
North American Frame 2								
na-eu*	–	–	–	–	–	–	0.224 ± 0.004	0.22 ± 0.01
na-eu	–0.038 ± 0.014	0.074 ± 0.004	0.243 ± 0.017	43.1	44.9	97.3	0.257 ± 0.015	–
na-pa*	–	–	–	–	–	–	0.820 ± 0.010	0.78 ± 0.01
na-pa	–0.128 ± 0.022	0.509 ± 0.008	–0.622 ± 0.010	75.0	–66.6	–83.8	0.814 ± 0.008	–
na-au*	–	–	–	–	–	–	0.810 ± 0.030	0.79 ± 0.01

Abbreviations are na, North American plate; eu, Eurasian plate; pa, Pacific plate; au, Australian plate. $\lvert\omega_0\rvert$ is the original rotation rates in NUVEL1 [*DeMets et al.*, 1990]. Units are deg/Ma (ω_x, ω_y, ω_z, $\lvert\omega\rvert$, $\lvert\omega_0\rvert$) and percent for correlations ($C_{x,y}$, $C_{y,z}$, $C_{z,x}$).
*Only the rotation rate was estimated.

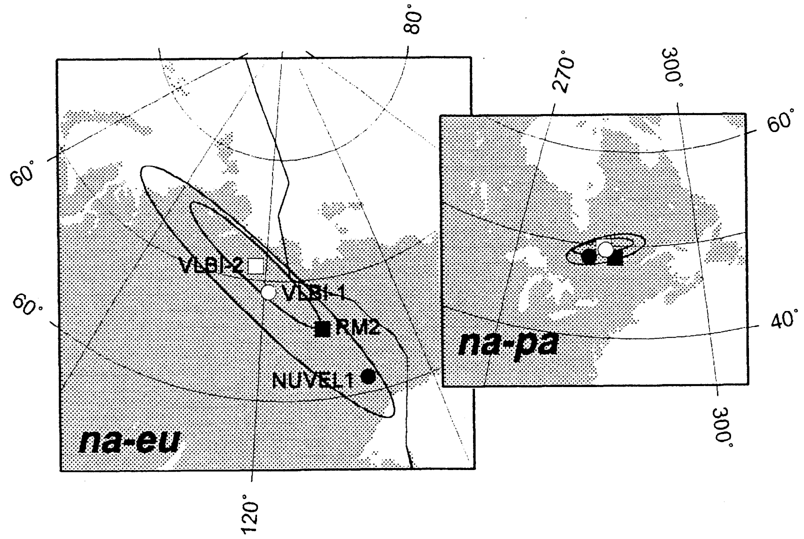

Figure 8. The positions and the 2σ error ellipses of the Euler poles for the North America–Eurasia (na–eu) and the North America–Pacific (na–pa) plate pairs, estimated by the KRFs based on the North American plate-fixed stations. Open circles and squares denote poles obtained using the North American Frame No. 1 (VLBI-1) and No. 2 (VLBI-2). Solid circles and squares denote those in the NUVEL1 [*DeMets et al.*, 1990] and RM2 [*Minster and Jordan*, 1978] models.

If the -4.5% revision [*DeMets et al.*, 1994] were correct, the present result would suggest (1) NUVEL1 gives the average movements over the last few millions of years, and individual Euler vectors over the last 10 years could be different from such averages, or (2) the original NUVEL1 rotation rates has a few percent uncertainties that have propagated from the observation errors of the raw data used in NUVEL1, and it is potentially difficult to discuss corrections of only a few percent. However, Figure 9 shows that three plate pairs require similar positive revision factors and favors an alternative possibility that the a priori revision coefficient of -4.5% is wrong. A recent study using the Doppler tracking measurement of the Doppler orbitography and radiopositioning integrated by satellite system also suggests plate velocities more consistent with the original NUVEL1 rather than the NUVEL1a [*Soudarin and Cazenave*, 1995], the same conclusion as the present study.

Conclusions

A method to redefine a KRF by translating and rotating the original KRF, that has been obtained with minimal necessary constraints, in three-dimensional space, has a potential of providing information on the vertical, as well as horizontal,

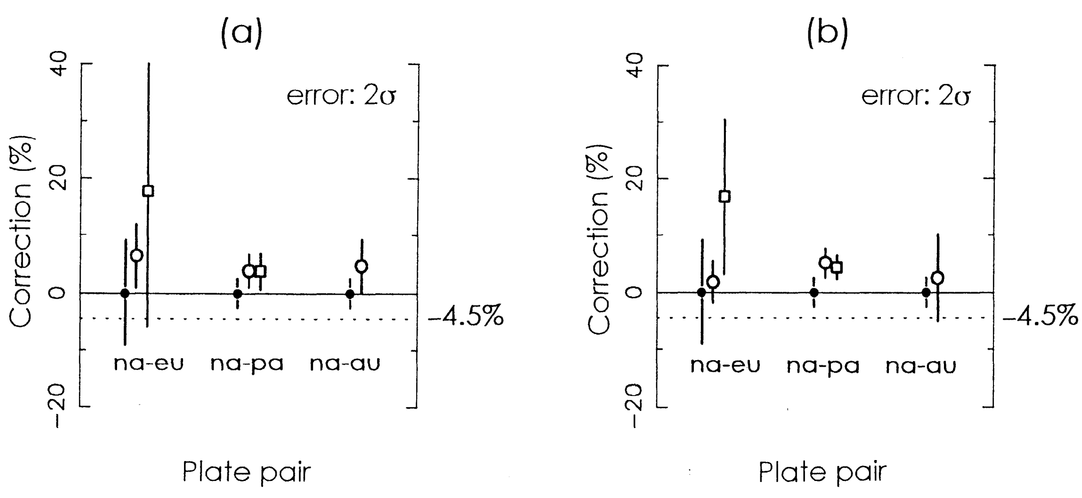

Figure 9. Comparisons of the NUVEL1 plate rotation rates (solid circles) and those estimated by VLBI data (open circles and squares) for the North America–Eurasia (na–eu), the North America–Pacific (na–pa), and the North America–Australia (na–au) plate pairs, obtained using the North American Frame (a) No. 1 and (b) No. 2. Error bars are 2σ. Rotation rates (vertical axis) are normalized by the original NUVEL1 rates. Open circles indicate the rates estimated as the only parameters, while squares indicate those estimated together with the rotation pole positions. Two VLBI stations on the Australian plates are too close to estimate the whole Euler vector. The a priori correction of -4.5% due to the astronomical calibration of the MPTS is shown as the dotted line.

site velocities. By adjusting only the horizontal velocities to the predictions, vertical velocities have been estimated in an objective manner. It is found that there is a certain correlation between the vertical velocities within stable plate interior in North America and the postglacial isostatic rebound model predictions. VLBI is beginning to detect vertical signals that are smaller than horizontal plate motions by an order of magnitude. No correlation was found, however, in Europe due to enigmatic 5~6 mm/yr subsidences of German stations. Although it is impossible to realize KRFs for all the tectonic plates, it is still possible to obtain velocities of plate boundary stations with respect to the plate interiors. However, we should consider hidden errors coming from the uncertainties of the reference plate motion model. I sought geodetic evidence supporting the -4.5% MPTS revision by directly estimating the correction coefficient for the original plate motion model and by estimating the Euler vectors for three pairs of tectonic plates. I conclude that such evidence is not to be found in the VLBI data from the last 10 years and consider it premature to use the NUVEL1a model in the standard terrestrial reference system without verifying it in a geodetic time window.

Acknowledgments. I thank Thomas A. Herring (MIT), Steven N. Ward (UCSC), Danan Dong (Caltech) and Kenneth Hudnut (Caltech) for their critical reviews of the manuscript. I owe much to Tom Herring who gave me a specific suggestion to my algorithm by showing the source code of his program. Discussions with John W. Robbins (Hughs STX) at EGS Hamburg and Christopher G. A. Harrison (University of Miami) at WPGM Hongkong contributed to this work. I also thank D. S. Caprette (GSFC) for uploading the GLB907 full covariance matrix file to CDDIS for my request, Harald Schuh (DGFI) for pointing out mistakes in the manuscript, Gill Foulger (University of Durham) for her advice in improving the English, and Yuko Ouchi for typesetting the manuscript. The software package, Generic Mapping Tool (GMT) version 3, was used to plot several of the figures in this paper.

References

Argus, D.F., and R.G. Gordon, Pacific-North American plate motion from very long baseline interferometry compared with motion inferred from magnetic anomalies, transform faults, and earthquake slip vectors, *J. Geophys. Res., 95*, 17,315–17,324, 1990.

Argus, D.F., and R.G. Gordon, No-net-rotation model of current plate velocities incorporating plate motion model NUVEL-1, *Geophys. Res. Lett., 18*, 2039–2042, 1991.

Avouac, J.-P., and P. Tapponnier, Kinematic model of active deformation in Central Asia, *Geophys. Res. Lett., 20*, 895–898, 1993.

Cande, S.C., and D.V. Kent, A new geomagnetic polarity time scale for the late Cretaceous and Cenozoic, *J. Geophys. Res., 97*, 13,917–13,951, 1992.

Caprette, D.S., C. Ma, and J.W. Ryan, Crustal dynamics project data analysis – 1990, VLBI geodetic results 1979–1989, *NASA Tech. Memo., 100765*, 1990.

DeMets, C., R.G. Gordon, D.F. Argus, and S. Stein, Current plate motions, *Geophys. J. Int., 101*, 425–478, 1990.

DeMets, C., R.G. Gordon, D.F. Argus, and S. Stein, Effect of recent revisions to the geomagnetic reversal time scale on estimates of current plate motions, *Geophys. Res. Lett., 21*, 2191–2194, 1994.

Douglas, B.C., Global sea level rise, *J. Geophys. Res., 96*, 6981–6992, 1991.

Dunn, P.J., M.H. Torrence, R. Kolenkiewicz, and D.E. Smith, Vertical positioning at laser observatories, in *Contributions of Space Geodesy to Geodynamics, Geophys. Monogr. Ser.*, vol. 23, edited by D.E. Smith and D.L. Turcotte, pp. 99–106, AGU, Washington, D. C., 1993.

Fallon, F.W., and W.H. Dillinger, Crustal velocities from geodetic very long baseline interferometry, *J. Geophys. Res., 97*, 7129–7136, 1992.

Geographical Survey Institute, Summary of observations for earthquake prediction in Japan, 2, Kanto and Chubu Areas, in *Special Report of the Regional Subcommittees of the Coordinating Committee for Earthquake Prediction* (in Japanese), vol. 4, pp. 43–94, Geogr. Surv. Inst., Minist. of Const., Tsukuba, Japan, 1994.

Gordon, R.G., Orbital dates and steady rates, *Nature, 364*, 760–761, 1993.

Gu, G.-H., and W.H. Prescott, Discussion on displacement analysis: Detection of crustal deformation, *J. Geophys. Res., 91*, 7439–7446, 1986.

Harland, W.B., A.V. Cox, P.G. Llewellyn, C.A.G. Pickton, A.G. Smith, and R. Walters, *A Geologic Time Scale*, Cambridge Univ. Press, New York, 1982.

Heki, K., Three approaches to improve the estimation accuracies of the vertical VLBI station positions, *J. Geod. Soc. Jpn., 36*, 143–154, 1990.

Hilgen, F.J., Astronomical calibration of Gauss to Matuyama sapropels in the Mediterranean and implication for the geomagnetic polarity time scale, *Earth Planet. Sci. Lett., 104*, 226–244, 1991a.

Hilgen, F.J., Extension of the astronomically calibrated (polarity) time scale to the Miocene/Plio-cene boundary, *Earth Planet. Sci. Lett., 107*, 349–368, 1991b.

Holt, W.E., M. Li, and A.J. Haines, Earthquake strain rates and instantaneous relative motions within Central and East Asia, *Geophys. J. Int., 122*, 569–593, 1995.

Houseman, G., and P. England, Crustal thickening versus lateral expulsion in the Indian-Asian continental collision, *J. Geophys. Res., 98*, 12,233–12,249, 1993.

James, T.S., and A. Lambert, A comparison of VLBI data with the ICE-3G glacial rebound model, *Geophys. Res. Lett., 20*, 871–874, 1993.

Jestin, F., P. Huchon, and J.M. Gaulier, The Somalia plate and the East African Rift System: Present-day kinematics, *Geophys. J. Int., 116*, 637–654, 1994.

Kato, T., Secular and earthquake-related vertical crustal movements in Japan as deduced from tidal records (1951-1981), *Tectonophysics, 97*, 183–200, 1983.

Ma, C., J.W. Ryan, and D.S. Caprette, NASA space geodesy program - GSFC data analysis – 1993, VLBI geodetic results 1979–92, *NASA Tech. Memo., 104605*, 1994a.

Ma, C., T.A. Clark, B.G. Bills, J.M. Gipson, and D.S. MacMillan, Vertical signatures observed in VLBI data (abstract), *Eos Trans. AGU, 75* (16), Spring Meet. Suppl., 105, 1994b.

Minster, J.B., and T.H. Jordan, Present-day plate motions, *J. Geophys. Res., 83*, 5331–5354, 1978.

Molnar, P., and P. Tapponnier, Cenozoic tectonics of Asia: Effects of a continental collision, *Science, 189*, 419-426, 1975.

Robaudo, S., and C.G.A. Harrison, Plate tectonics from SLR and VLBI global data, in *Contributions of Space Geodesy to Geodynamics, Geophys. Monogr. Ser.*, vol. 23, edited by D.E. Smith and D.L. Turcotte, pp. 51–71, AGU, Washington, D. C., 1993a.

Robaudo, S., and C.G.A. Harrison, Measurements of strain at plate boundaries using space based geodetic techniques, *Geophys. Res. Lett., 20*, 1811–1814, 1993b.

Robbins, J.W., D.E. Smith, and C. Ma, Horizontal crustal deformation and large scale plate motions inferred from space geodetic techniques, in *Contributions of Space Geodesy to Geodynamics, Geophys. Monogr. Ser.*, vol. 23, edited by D.E. Smith and D.L. Turcotte, pp. 21–36, AGU, Washington, D. C., 1993.

Segall, P., and M.V. Matthews, Displacement calculations from geodetic data and the testing of geophysical deformation models, *J. Geophys. Res., 93*, 14,954–14,966, 1988.

Shackleton, N.J., A. Berger, and W.R. Peltier, An alternative astronomical calibration of the lower Pleistocene time scale based on ODP Site 677, *Trans. R. Soc. Edinburgh Earth Sci., 81*, 251–261, 1990.

Soudarin, L., and A. Cazenave, Large-scale tectonic plate motions measured with the DORIS space geodesy system, *Geophys. Res. Lett., 22*, 469–472, 1995.

Sun, F.-P., and M. Zhao, An instantaneous plate motion model from integrated VLBI and SLR data, *J. Geod. Soc. Jpn., 40*, 107–111, 1994.

Tushingham, A.M., and W.R. Peltier, ICE-3G: A new global model of late Pleistocene deglaciation based upon geophysical predictions of postglacial relative sea level change, *J. Geophys. Res.*, *96*, 4497–4523, 1991.

Ward, S.N., North America-Pacific plate motions: New results from very long baseline interferometry, *J. Geophys. Res.*, *95*, 21,965–21,981, 1990.

Watkins, M.M., R.J. Eanes, and C. Ma, Comparison of terrestrial reference from velocities determined from SLR and VLBI, *Geophys. Res. Lett.*, *21*, 169–172, 1994.

K. Heki, Division of Earth Rotaion, National Astronomical Observatory, 2-12 Hoshigaoka, Mizusawa, Iwate 023, Japan. (e-mail: heki@miz.nao.ac.jp)

(Received December 2, 1994; revised September 8, 1995; accepted September 13, 1995.)